PREPRINT UCRL-78579

CONF-760513--11

Lawrence Livermore Laboratory

DESIGN TECHNIQUES AND MEASURED PERFORMANCE FOR A UNIFORMLY-PUMPED 4-CM DIAMETER ROD AMPLIFIER

G. J. Linford and S. M. Yarema

June 30, 1976

This paper was prepared for submission to
Conference on Laser and Electro-Optical Systems
San Diego, CA, May 25 - 27, 1976

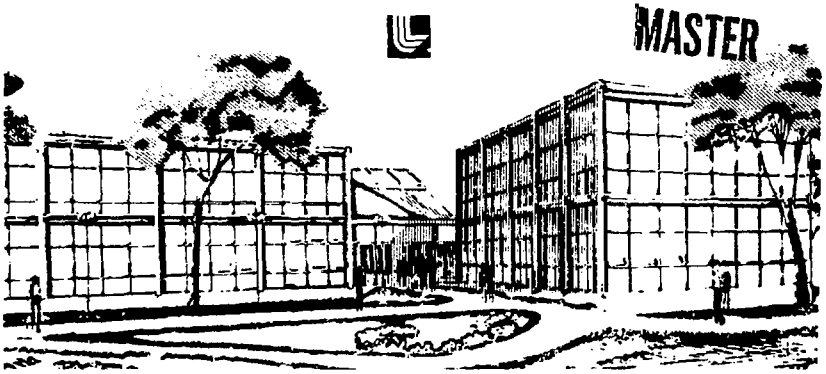

DESIGN TECHNIQUES AND MEASURED PERFORMANCE FOR A UNIFORMLY-PUMPED 4-CM DIAMETER ROD AMPLIFIER*

G. J. Linford and S. M. Yarema

Lawrence Livermore Laboratory
University of California
P.O. Box 808
Livermore, CA 94550

ABSTRACT

A solid-state laser rod amplifier of moderate aperture achieving a high degree of spatial gain uniformity has been constructed and its performance evaluated. Digital and analogue techniques were used to optimize the amplifier design for performance in a laser fusion application. Results of simple 2-D computer simulations and experimental evaluations of amplifier performance are presented.

*Work performed under the auspices of the U.S. Energy Research & Development Administration under contract No. W-7405-Eng-48.

OT W-7405-ENG-48 EJ

DESIGN TECHNIQUES AND MEASURED PERFORMANCE FOR A UNIFORMLY-PUMPED 4-CM DIAMETER ROD AMPLIFIER

G. J. Linford and S. M. Yarema

Lawrence Livermore Laboratory
P.O. Box 808
Livermore, CA 94550

I. INTRODUCTION AND SUMMARY

Laser amplifiers designed for use in high-radiance laser fusion systems must meet stringent requirements with regard to their non-linear phase shifts, optical gain uniformity, control of parasitic oscillations, and optical phase distortions. Since the intensity profile of the laser beam directly affects the illumination uniformity (and hence the implosion symmetries) of laser fusion targets, it is essential that the individual laser amplifiers in each amplifier chain have high gain and highly uniform gain distributions. For large aperture glass laser rod amplifiers, this is difficult to achieve since the pumping radiation from the flashlamps must pass through the outer portions of the laser rod before the axis can be pumped.

Our analyses of the pumping cavity geometry have indicated that there are approximately twelve pertinent parameters which must be considered in performing an n-dimensional optimization analysis of the pumping cavity. Simple two-(spatial) dimensional digital computer ray-tracing simulations were used to identify n-space saddles, and analogue techniques corroborated and normalized the indicated maxima and minima.

Using these methods, we have designed and constructed a 4-cm diameter laser amplifier which as a (linear) gain uniformity of $\pm$ 5% across its full aperture. This amplifier achieved a measured CW gain of 9.5 $\pm$ 0.5 at an input energy of 12 kJ to six 1.3 cm-bore CFQ lamps

having a xenon pressure of 300 Torr. The 0.3% Nd^{+++}-doped 4x25 cm laser rod was jacketed with a samarium-doped shield glass of 6-cm diameter filled with a nearly-saturated solution of $ZnCl_2$ and water (n=1.53) to match the refractive index (n=1.556) of the silicate laser rod. This jacket enhanced the optical efficiency of the pumping cavity while controlling the spurious parasitic and fluorescent depumping mechanisms present in an unclad glass rod. The elliptical reflectors were of eccentricity 0.52, and the foci of each segment were centered on the rod and flashlamp axes respectively.

II. DEFINITION OF OPTIMIZATION PARAMETERS

Each of the four major laser rod amplifier requirements defined above will be discussed briefly below in the context of our optimization analysis.

A. Non-Linear Phase Shift Contributions

The non-linear phase shifts produced by the passage of a high intensity beam through a dielectric material introduce (1) whole beam phase retardations proportional to the product of non-linear index and beam intensity (and having, therefore, a similar spatial profile), (2) small-scale beam break-up according to the Bespalov-Talanov theory[1], and (3) damage to bulk material and/or dielectric-coatings if limitations on peak beam intensity, modulation, and damage thresholds are not met.. Each of these effects is discussed in detail elsewhere,[2] and only a brief review will be presented here.

The non-linear phase shift (in nepers) produced by a passive dielectric element of thickness L (cm) placed in a spatially homogeneous beam of flux I (watts/cm^2) and wavelength λ_{vac} (cm)

is given by

$$B(r) = \frac{2\pi}{\lambda_{vac}} \int_0^L n_2 I(r) dz \qquad (1)$$

where n_2 is the non-linear refractive index, r is the radial coordinate perpendicular to the direction of propagation and z is parallel to the axis of the laser amplifier (for a typical silicate laser glass, $\frac{2\pi}{\lambda} n_2 = 2.4 \times 10^{7}$ cm/W). Inside a rod amplifier, the optical flux in the beam is increasing exponentially as it passes through the rod so that

$$B(r) = \frac{2\pi}{\lambda_{vac}} \int_0^L I(r)_{in}\, n_2 \exp(\sigma N z)\, dz \qquad (2)$$

which is easily integrated to produce

$$B(r) = \frac{8}{\lambda_{vac}} n_2 \frac{(G - 1)}{\ln G} L \frac{P_{in}(r)}{D^2} \qquad (3)$$

where G is the optical power gain, P_{in} (watts) is the input power, and D is the diameter of the laser beam passing through the laser amplifier. The optical power gain, G, is defined in terms of the stimulated emission cross-section, σ, the population inversion density, N, and rod length, L, by the expression

$$G = \exp(\sigma NL) \qquad (4)$$

From equation (3), it is evident that to minimize B for constant P_{in}, G and D must be maximized while holding L to a minimum. Selections of suitable materials for laser rod amplifiers fixes the values of λ_{vac}, σ, and n_2.

B. Achievement of Maximum Gain

From equation (4), it is apparent that the maximum gain in a given laser rod amplifier can be achieved by maximizing the inversion density, N. This can be achieved by (1) optimizing the optical efficiency of the pumping cavity, (2) maximizing the amount of optical power available in the pumping bands of the laser rod,and (3) suppressing deoumping mechanisms within the rod amplifier.

The most efficient pumping cavity uses a large, elliptical reflector cylinder having very high specular reflectivity in the pumping bands of the solid-state laser material. A linear flashlamp of optimized bore and energy loading is placed at one of the cylindrical foci whereas the axis of the laser rod is placed at the other focus. Unfortunately, limitations on the explosion energy of a single flashlamp force the selection of a multi-lamp cavity at the expense of a loss in efficiency.

Control of spurious parasitic oscillations is also necessary in order to prevent loss of population inversion. Optically efficient elliptical cylinders used in pumping cavities present potentially serious parasitic problems since they couple fluorescent radiation from the laser rod back into the rod after one transit through the flashlamp focus. As discussed below, use of a suitable absorbing ion in either the laser rod shield glass or in the immersion fluid will permit the selective attenuation of the fluorescent line(s), thereby preventing the onset of this class of spurious parasitic modes.

For many laser chain applications, no change in the intensity profile of the amplified laser beam is desired, and hence the radial and azimuthal gain variations in the rod amplifier must be minimized. This latter requirement vastly complicates the design of the pumping cavity, and generates the need for both analog and digital computations to assist in probing the parameter space.

C. Control of Parasitic Oscillations

Control of parasitic oscillations is achieved by increasing the optical losses associated with the various types of parasitic modes.

1. "Whisper Modes"

Since an unclad laser rod is bounded by a dielectric discontinuity of (n-1), total internal reflections (TIR) can take place for all interior angles of incidence satisfying the inequality:

$$\theta' \leq \sin^{-1}(1/n) \qquad (5)$$

As indicated in Figure 1, parasitic modes (so-called "whisper modes") suffer very small losses within the annular volume bounded by d/n and d of an unclad rod of diameter d. Use of a shield glass of diameter $d' = nd$ concentric with the laser rod and filled with an index-matching fluid[3] transparent to the pumping radiation forces the "whisper modes" completely out of the laser rod.[4] Doping either the immersing fluid or the shield glass itself with an ion suitable for absorbing the fluorescent line(s) of the laser rod can introduce sufficient losses such that parasitic oscillations fall below threshold. We experimented with both samarium-doped shield glasses and samarium chloride salt in the immersion

fluid and found both methods to be suitable for suppressing the 1.062 μm and 1.33 μm fluorescent lines in Nd:glass. The index-matching fluid (saturated solution of $ZnCl_2$) also enhanced the pumping efficiency of the laser rod, permitting the entire volume[4] of the laser rod to be accessible from the flashlamp cavity.

D. Control of Optical Phase Distortion

Assuming that the laser rod is initially free of strain birefringence, striae, seeds, bubbles, and defects in the figuring of the two (parallel) end faces, two major mechanisms within the laser rod amplifier can impair the optical phase distortion and polarization state of the output beam: (1) anisotropic heating (or cooling) of the laser rod shortly after the lamps have been fired, or (2) excessive pressure on the rod produced by the mounting assemblies. Flowing the index-matching fluid through a heat exchanger permits much of the heat to be removed from the laser rod, thereby reducing the time delay required between successive firings of the flashlamps. Acceptable levels of stress birefringence were measured by inspecting the assembled rod amplifier with a full-aperture polariscope.

III. COMPUTER SIMULATION OF PUMPING CAVITY

A relatively simple 2-D Monte-Carlo ray-tracing code (MIR28)[5] was used to probe the n-dimensional pumping cavity parameter space. As shown in Figure 1, the "unit cell" used in these computations was a "pie slice" of the actual pumping cavity geometry under consideration. The computer program ray-traced the rays emanating from a semi-opaque flashlamp plasma

column, reflecting them from the walls of the reflector and from the radial segments of the unit cell. The laser rod and shield glass assembly were divided into radial zones, and the calculated energy intercepted by each zone plotted as a function of the radius from the center of the rod.

A. Definition of Optimization Parameters

Twelve parameters were considered in calculating the focusing efficiencies of various pumping cavity geometries. They were:

1. product of active ion doping (Nd^{+++}) and laser rod diameter,
2. refractive index of immersion fluid,
3. flashlamp opacity,
4. lamp circle diameter,
5. flashlamp bore,
6. distance from lamp to reflector,
7. number of flashlamps,
8. reflector eccentricity,
9. locations of reflector foci,
10. uv, visible, and ir reflectivities of flashlamp reflector,
11. absorption coefficient of shield immersion fluid, and
12. displacement of the lamp from the reflector-segment axis.

At its current stage of development, our 2-D ray-tracing code does not include the effects of refraction at the flashlamp/N_2 or shield glass/N_2 interfaces. This omission is judged to produce only a small error in the ray tracing intensities at nearly-normal incidence.

Design requirements, simplifications, and obvious trade-offs among these twelve pumping cavity parameters reduce the labor somewhat in

finding the n-space saddle points. Thus, for example, the lamp circle is restricted to values greater than the sum of the shield glass radius and the semi-diameter of the flashlamp, the product of doping and rod diameter is kept in the range of 3%-cm to 5%-cm, etc.

The 2-D ray-tracing computer code was used exclusively to compare pumping cavity geometries with no attempt being made to calculate the specific geometrical parameters associated with the optimum geometry. Four different reflector designs were constructed and tested. Data regarding the resultant gain profiles produced by these four reflectors were used to normalize the computer calculations. The geometrical properties of these four reflectors are summarized below in Table I.

Major emphasis was given attaining a highly uniform gain profile across the rod amplifier aperture. The initial reflector design, reflector #1 (see Table I for a summary of the reflector properties), was selected on the basis of satisfying the optical pumping power requirements of the laser. As shown in Figure 2, the gain profile achieved with reflector #4 achieves a variation of only $\pm$ 3% in gain coefficient from center to edge of the rod amplifier. For comparison, the unnormalized computer simulations of these four geometries are shown in Figure 3. As shown, the 2-D ray-tracing code alone does not correctly predict the measured gain profiles, although it was able to place the four reflector geometries in the correct order with regard to their relative abilities to focus flashlamp illumination directly into the center of the rod amplifier. Thus, the role of the 2-D program in our optimization study was as a tool to compare a very large number

of relatively similar designs. The final arbiter, however, was the construction of specific reflector designs and testing them in the prototype amplifier chassis.

B. Effect of Doping on Rod Amplifier Gain Profiles

Measurements[6] made of the absorption of xenon flashlamp light by Nd^{+++}:doped silicate laser glass of different dopings were used to permit our 2-D computer simulations to estimate the differences in gain profiles produced when rods of different dopings were installed in the optimized laser amplifier. Figure 4 illustrates the gain profiles obtained when 3% and 0.8%-Nd-doped laser rods were installed in our optimized laser amplifier. The higher-doped laser rod, as predicted, displays a higher gain at the edge owing to the higher absorption coefficients of the more heavily-doped laser glass.

IV. DESCRIPTION OF EXPERIMENTAL MEASUREMENTS

Three general types of measurements were made on the prototype rod amplifier:

1. flashlamp measurements (current waveform, stored energy),
2. gain measurements (small signal, gain profile, time development), and
3. optical measurements (optical phase distortion, strain, stress birefringence, reflectivity of coatings, refractive indices of immersion fluid, absorption of salt solutions at 1.062 and 1.33 μm).

The flashlamp measurements were made to verify that the flashlamp pulse lengths were appropriate, that the pulse-forming-network was damped

properly, and that the optical power delivered to the pumping cavity was known. The gain measurements permitted the attainment of a uniform gain profile by varying the geometry of the pumping cavity in accordance with the parametric optimization furnished by the 2-D computer simulation. These gain measurements also demonstrated that dynamic apodization of the laser beam was possible with the radially symmetric gain profiles obtained using 12-lobe (#1) reflectors. Optical measurements permitted us to verify that refractive indices and component absorptions were acceptably close to the required values for the gain measurement experiments.

A. Description of Gain Measurement Apparatus

The small signal, CW optical power gain of the rod amplifier was measured using a small (0.2 cm diameter), 0.5 watt CW probe laser beam from a Nd:YAG laser. As shown in Figure 5, the beam was centered on the axis of the rod amplifier using a pair of cross-hairs designed to fit snugly into the input and exit apertures of the CW amplifier. A beam-splitter directed a portion of the incident CW laser beam around the amplifier to permit the time variation of the laser output power to be monitored. A second photodiode was used to monitor the output power from the rod amplifier itself. In this manner, it was possible to measure the small-signal amplifier gain at various points within the amplifier aperture to an accuracy of $\pm$ 1%. These measurements were made with the time response of the photodiode circuits sufficiently fast to record the time development of the laser amplifier gain from the flashlamp trigger to the peak of fluorescence.

B. Effect of Flashlamp Bore on Gain Profiles

Two lamp bores were used in these experiments: 0.5 and 1.3 cm. As shown in Figure 6, the effect produced by reducing the flashlamp bore primarily resulted in a more strongly-focussed pumping cavity, as expected from the use of elliptical reflector segments.

C. Effect of Immersion Fluid Refractive Index on Gain Profiles

Refractive indices ranging from 1.00 to 1.53 were examined to determine the effect produced on the gain profile of the rod amplifier. Figure 7 illustrates the results obtained when immersion fluids having indices ranging from 1.00 (dry nitrogen) to 1.53 (saturated $ZnCl_2$ solution) were used in a pumping cavity using a 12-lobe reflector. Figure 8 demonstrates the effects produced in a 6-lobe cavity as the refractive index is changed. Since reduction of the refractive index below that of the silicate laser glass permits a fraction of the laser rod volume to be swept out by parasitic "whisper" modes (when no fluorescence absorber is present), it permits various gain profiles to be achieved in the rod amplifier for dynamic apodization applications. This property is also available using various bore flashlamps, although it must be emphasized that smaller bore flashlamps have substantially shorter lifetimes when operated at the same input energy.

D. Effect of Flashlamp Reflector Material on Gain Profile

Two types of reflector material were used in these experiments: crenulated polished aluminum sheet and silver-plated brass or copper. As shown in Figure 2, not only is the efficiency higher for the silver-plated 6-lobe reflector, but the shapes of the gain profiles

are different for the two 6-lobe reflectors: thus, since the silver reflector has a higher reflectivity in the Nd:glass pumping bands than does the polished aluminum reflector, it is more successful at focusing pumping radiation into the interior of the laser rod. The higher uv reflectivity of the aluminum is actually a disadvantage in the case of Nd:glass since it results in an increased heat load on the glass without a proportional increase in useful pumping light.

E. Influence of Input Energy on Gain Profile

As indicated in Equation (4), the gain of the rod amplifier is proportional to the population inversion density, N, which, in turn, is approximately proportional to the input power in the flashlamps (in the absence of significant parasitic oscillations). Thus, the gain coefficient of the rod amplifier should be linearly proportional to the input energy to the flashlamps. As shown in Figure 9, this proportionality was actually observed for input energies ranging from 6 kJ to 13.7 kJ.

F. Details of 4x25 cm Rod Amplifier Assembly

The heart of the 4-cm rod amplifier is a 4x25 cm silicate-glass laser rod. The quasi-parallel plane ends of the laser rod are coated with a multi-layer "V" anti-reflection (AR) coating. Only 20 cm of the laser rod is exposed to direct flashlamp illumination; the remaining 2.5 cm at each end is used to seat "O" rings for the liquid immersion system. As shown in Figure 1, a cylindrical shield glass is mounted concentric with the rod axis. The radius of the shield glass is mounted concentric with the rod axis. The radius of the shield glass was selected to be approximately n times the rod

radius ($n_{silicate}$=1.556) to permit the control of so-called "whisper modes" and increase the pumping efficiency of the laser rod. Galleries internal to the amplifier end bells permitted the $ZnCl_2$ index-matching immersion fluid to be circulated through a temperature-controlled heat exchanger/fluid reservoir. Both Pyrex and samarium-doped soda-lime glass shield glasses were used (the former required use of $SmCl_3$ in the $ZnCl_2$ immersion fluid). The radius of the flashlamp circle is 4.52 cm, and six 300 Torr xenon flashlamps having bores of 1.3 cm were used.

The $ZnCl_2$ fluid is viscous (25 poise) and requires generous pump capacities and relatively large fluid galleries in order to be circulated at an acceptable flow rate (several cm^3/sec). One per cent hydrochloric acid is added in order to prevent the precipitation of white zinc-hydroxide ($ZnCl_2 \cdot 4Zn(OH)_2$) under the influence of uv light from the flashlamps.

G. Explosion Energies of Flashlamps

Limitations on the maximum attainable gain of the 4-cm rod amplifier studied in these experiments are imposed by the explosion energies of the xenon flashlamps. Data on the 300 Torr, 1.3 cm bore lamps having 20 cm arc lengths indicate that the anticipated lifetime for these lamps is 2×10^4 shots @ an input energy to each lamp of 2.0 kJ. Additional values are summarized in Table II, below.

TABLE II

Variation of Flashlamp Lifetime with Input Energy

#	Input Energy	Estimated Lifetime	Fraction of Explosion Energy
1	1.0 kJ	6×10^5	11%
2	1.5 kJ	8×10^4	17%
3	2.0 kJ	2×10^4	22%
4	2.5 kJ	6×10^3	28%
5	3.0 kJ	10^3	33%

V. CONCLUSIONS

A methodology has been developed which permits laser pumping cavities to be configured in such a manner that specific pumping distributions within a solid-state laser rod can be obtained. For laser chain applications, a uniform gain profile is desirable, and the techniques described above have been used to change an initially anisotropic gain distribution into a relatively homogeneous gain distribution for a 4-cm diameter laser rod of relatively low Nd^{+++} doping (0.8%). Control of spurious parasitics in the laser amplifier was achieved by using samarium-doped index-matching shields. Ultimate limitations on the maximum attainable gain is caused by the explosion energies of the flashlamps.

ACKNOWLEDGEMENTS

The authors would like to acknowledge the substantial assistance given them by S. Guch in designing and constructing the 4-cm amplifier prototype. They would also like to thank E. J. Goodwin for developing the MIR28 2-D computer program used in calculating the theoretical energy depositions.

REFERENCES

1. V. I. Bespalov and V. I. Talanov, JETP Letters, 3, 307 (1966).

2. Laser Program Annual Report 1974, UCRL-50021-74, pp. 178-203, LLL, University of California, March 1975.

3. J. Linn, Applied Optics, 4, 1099 (1965).

4. G. J. Linford and L. W. Hill, Applied Optics, 13, 1387 (1974).

5. E. Goodwin, "MIR28" Computer Program, LLL. University of Calif., 1975.

6. J. Holzrichter, Unpublished Communication, SSL-73-321, LLL, University of Calif. 1973.

CROSS-SECTION OF LASER ROD AMPLIFIER

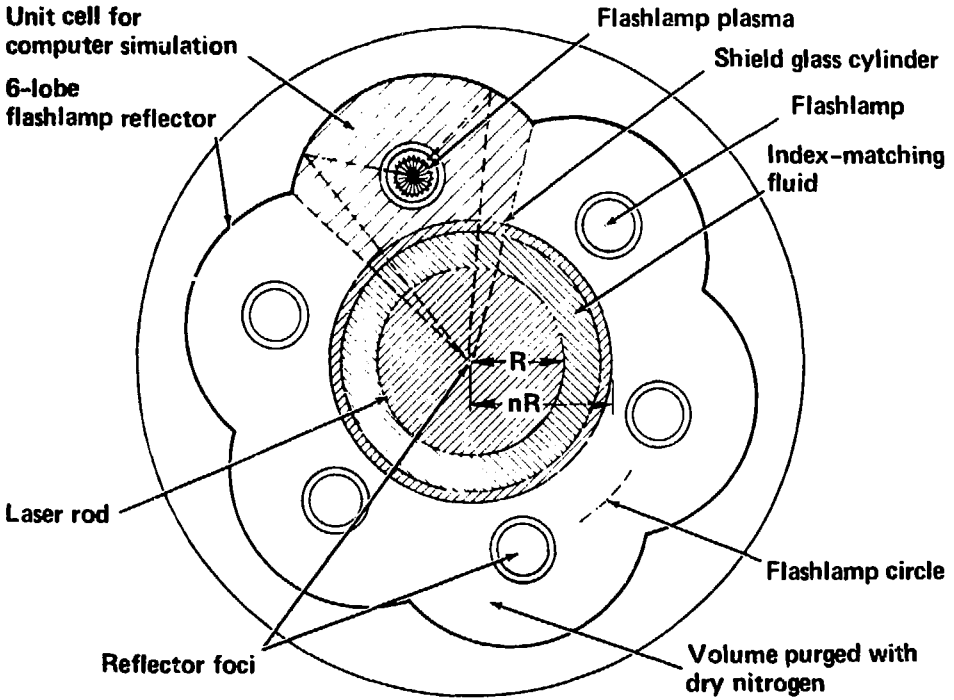

Fig. 1

MEASURED GAIN PROFILES FOR REFLECTORS #1,2,3, and 4

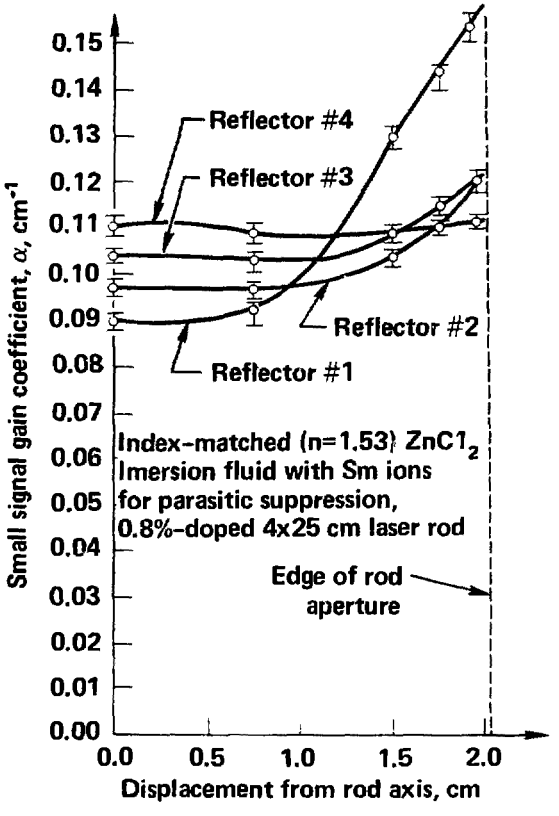

Fig. 2

COMPUTED (UNNORMALIZED) ENERGY DEPOSITION PROFILES FOR 4-cm ROD AMPLIFIER REFLECTORS (MIR28 SIMULATION)

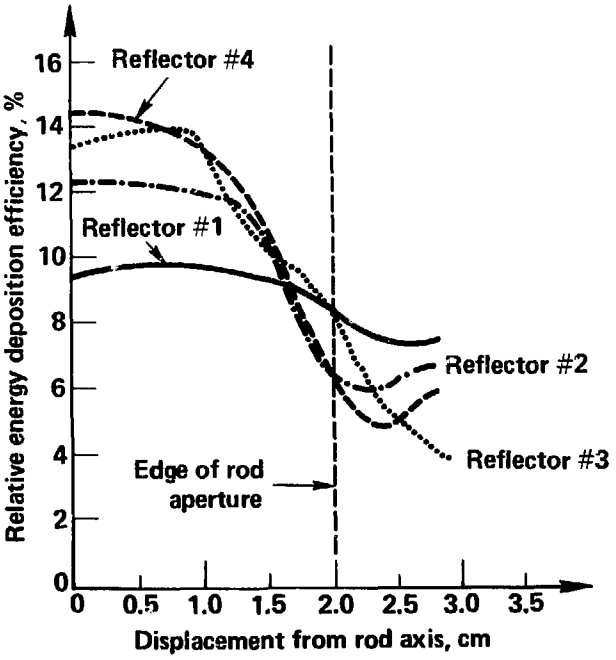

Fig. 3

GAIN PROFILES FOR 0.8% and 3.0%-Nd^{+++} -DOPED 4x25 cm LASER RODS IN OPTIMIZED PUMPING CAVITY

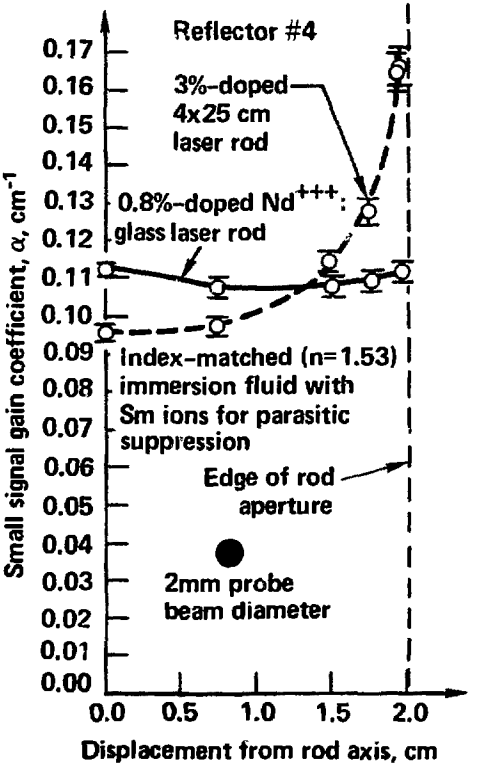

Fig. 4

SCHEMATIC OF GAIN MEASUREMENT APPARATUS

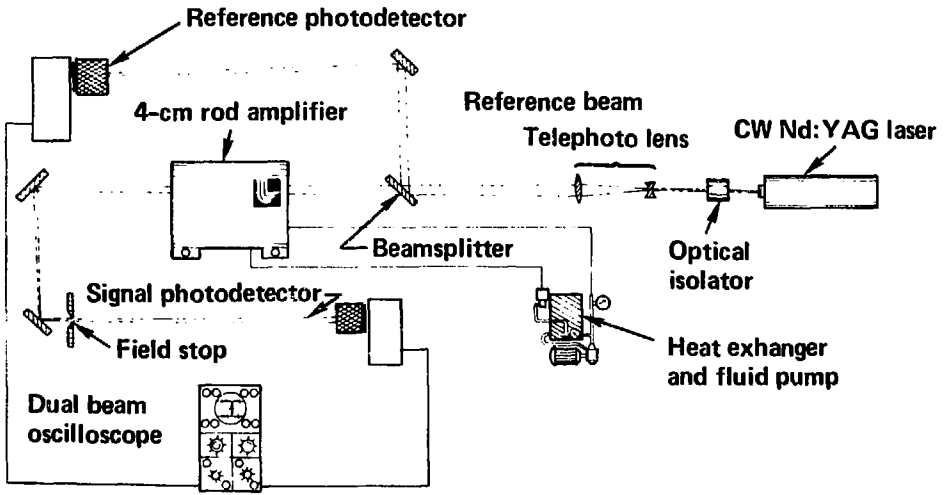

Fig. 5

GAIN PROFILES OF 4-cm ROD AMPLIFIER AS FUNCTIONS OF FLASHLAMP BORE

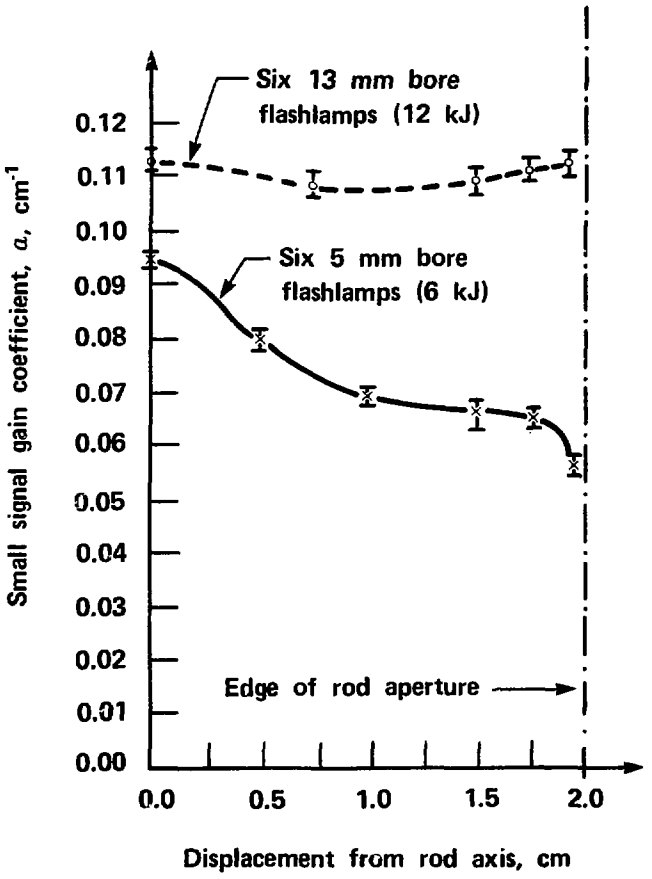

Fig. 6

GAIN PROFILES OF 4-cm ROD AMPLIFIER AS A FUNCTION OF IMMERSION FLUID PARAMETERS– 12-LOBE REFLECTOR #1

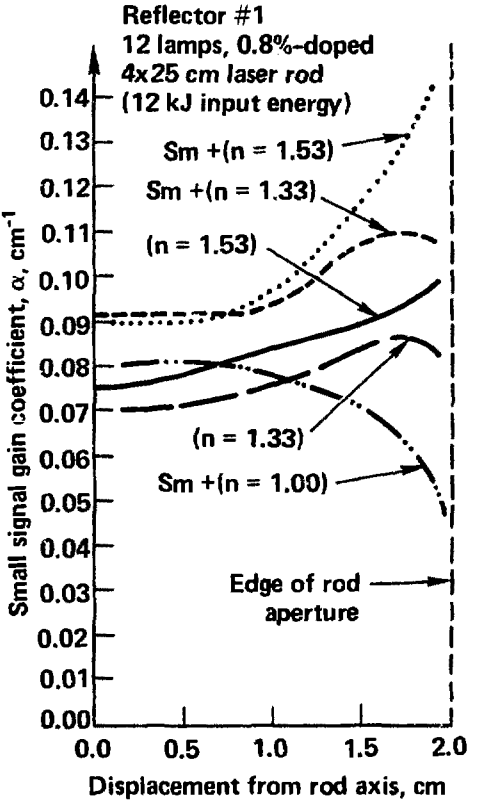

Fig. 7

GAIN PROFILES OF 4-cm ROD AMPLIFIER AS A FUNCTION OF IMMERSION FLUID REFRACTIVE INDEX-REFLECTOR #4

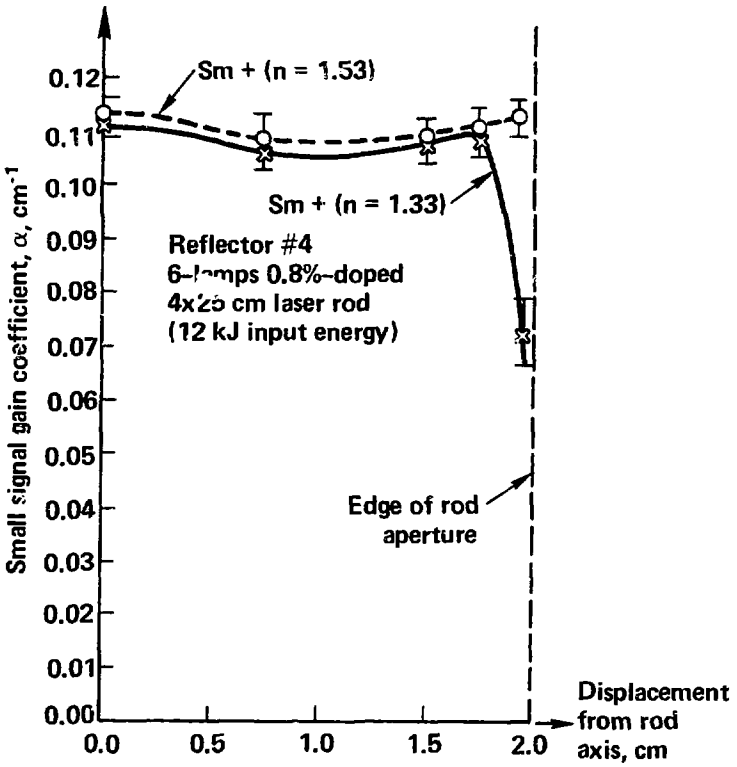

Fig. 8

VARIATION OF GAIN COEFFICIENT PROFILE WITH INPUT ENERGY TO 4 × 25 cm ROD AMPLIFIER

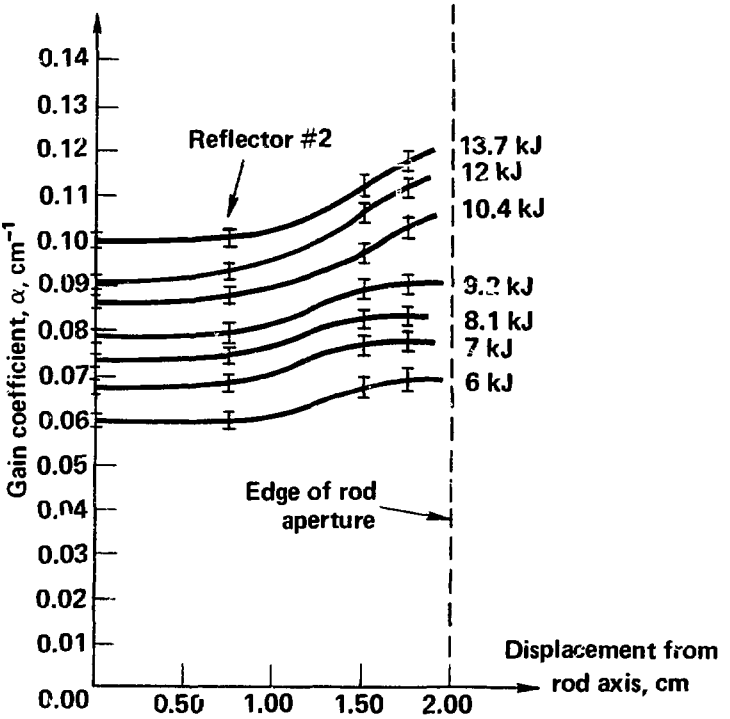

Fig. 9